Downloaded from rsta.royalsocietypublishing.org

PHILOSOPHICAL TRANSACTIONS OF THE ROYAL SOCIETY A MATHEMATICAL, PHYSICAL & ENGINEERING SCIENCES

Surface Properties in an External Electric Field [and Discussion]

J. E. Inglesfield, D. Weaire, J. E. Inglesfield, O. K. Andersen, U. Gerhardt and V. Heine

Phil. Trans. R. Soc. Lond. A 1991 **334**, 527-538
doi: 10.1098/rsta.1991.0032

Email alerting service

Receive free email alerts when new articles cite this article - sign up in the box at the top right-hand corner of the article or click **here**

To subscribe to *Phil. Trans. R. Soc. Lond. A* go to:
http://rsta.royalsocietypublishing.org/subscriptions

This journal is © 1991 The Royal Society

Downloaded from rsta.royalsocietypublishing.org

Surface properties in an external electric field

By J. E. Inglesfield

Institute for Theoretical Physics, Catholic University of Nijmegen, Toernooiveld, NL-6525 ED Nijmegen, The Netherlands

This paper reviews recent calculations on the effect of an external electric field on surface electronic properties, in particular using the embedding method for solving the Schrödinger equation at the surface. The shape of the screening charge and its field dependence are discussed, and the results are compared with experiments in which the image plane is determined. The force on the surface atoms in the field is given in terms of an effective charge, which also determines the work-function variation with surface displacements. This relationship can lead to a surface instability if the effective charge is big enough.

1. Introduction

In this paper I discuss recent calculations on the effect of an external field on a metal surface. Classically we know what happens: the field is perfectly screened, with a surface charge density of $\mathscr{E}/4\pi$. However, the microscopic details of the screening are important for many problems in surface science (Inglesfield 1990): in the field emission and field ion microscopes, and the scanning tunnelling microscope, an electric field is applied to the surface, and in electrochemistry there is a strong field across the Helmholtz double layer at the surface of the electrode (Kolb *et al.* 1981). The centre of gravity of the screening charge (averaged across a plane parallel to the surface) corresponds to the reference plane for the image potential (Lang & Kohn 1973), of current interest given the data available from inverse photoemission experiments on the energies of the image-potential-induced surface states (Smith *et al.* 1989). Nonlinear effects in screening, manifesting themselves as a change in the shape of the screening charge with field strength, show up in second harmonic generation when laser light is reflected from the surface (though our results for the screening of a static field can only be applied in the low-frequency limit (Weber & Liebsch 1987*a*)).

The atoms themselves respond to an external field; the net force on the metal is, after all, $\mathscr{E}^2/8\pi$ per unit area. But once again a detailed description of the forces on the atoms must be important for understanding the process of field evaporation where surface atoms are stripped off by a strong field: on the W (001) surface, for example, preferential field evaporation occurs in field ion experiments, removing alternate atoms to give a $(\sqrt{2}\times\sqrt{2})R45°$ vacancy structure (Melmeed *et al.* 1979). Computations show that an external field can induce a (1×2) reconstruction of the Ag (110) surface (Fu & Ho 1989), suggesting that the effect of alkali adsorbates in driving this reconstruction is due to an excess surface charge resulting from alkali ionization, analogous to the screening charge in the external field. Another example of surface atoms responding to an external field is in electron energy loss (EELS) experiments, where surface phonons are excited by low-energy electrons: in the

Phil. Trans. R. Soc. Lond. A (1991) **334**, 527–538
Printed in Great Britain

The Royal Society is collaborating with JSTOR to digitize, preserve, and extend access to *Philosophical Transactions: Physical Sciences and Engineering.* www.jstor.org

Downloaded from rsta.royalsocietypublishing.org

dipole scattering régime this can be discussed in terms of effective charges on the surface atoms.

In §§2 and 3 I review calculations of the screening charge for different surfaces, and use this to discuss experimental results on image potentials and second harmonic generation. The calculations involve the self-consistent solution of the electronic Schrödinger equation with surface geometry, and I describe in particular the embedding method (Inglesfield & Benesh 1988) which can be used to find the electronic states at the surface of a semi-infinite solid as an alternative to the more widely used slab geometry (Krakauer *et al.* 1979). To discuss forces on surface atoms in the presence of a field I discuss the concept of effective charges in §4, and then use this in §5 to discuss a surface instability driven by effective charges and its possible application to O chemisorbed on Cu (001).

2. Surface electronic structure in an external field

The first calculations of the screening of an external field at a surface were carried out by Lang & Kohn (1970), for free-electron-like metal surfaces modelled by semi-infinite jellium. Like (almost) all subsequent surface calculations, this was carried out within the mean-field framework of density functional theory; in addition to the Hartree and external potentials, an electron feels an exchange-correlation potential to describe the effects of exchange and the correlated motion of the electrons. The exchange-correlation potential $V_{\rm xc}$ is local and energy independent, and it can be found quite accurately using the local density approximation – $V_{\rm xc}(\boldsymbol{r})$ is taken as the exchange-correlation potential of a uniform electron gas with the density of electrons at $\boldsymbol{r}$. As the Hartree and exchange-correlation potentials depend on the electron density, this has to be found self-consistently; in the presence of an external field, the screening charge drops out automatically in the process of iterating to self-consistency. Solving the one-electron Schrödinger equation itself is relatively straightforward for the jellium surface, because the potential is one-dimensional and it is easy to match the wavefunctions in the surface region onto the bulk solutions (Lang & Kohn 1970). Jellium calculations are still extremely useful in studying surface response, especially the frequency-dependent response for which they are the only feasible calculation at present, and Liebsch and his co-workers have discussed second harmonic generation in this way (Weber & Liebsch 1987*a*, *b*; Liebsch & Schaich 1989). However, we shall see in §3 that there are very significant differences in (static) screening when the atoms are taken into account.

In general it is more difficult to solve the Schrödinger equation at the surface than in the bulk, because of the absence of translational symmetry in the direction perpendicular to the surface: only the Bloch wavevector $\boldsymbol{K}$ parallel to the surface is a good quantum number. In principle it can be done using the generalization of Lang & Kohn's (1970) wavefunction matching to the three-dimensional case. As Heine has shown (1963), there is a one-to-one relationship between the solutions of the bulk Schrödinger equation, travelling towards or away from the surface at energy E and with wavevector component $\boldsymbol{K}$, and the surface reciprocal lattice vectors $\boldsymbol{G}$. This means that there are exactly the right number of bulk solutions for matching onto a surface solution in amplitude and derivative, assuming that these are expanded as a Fourier series in $\boldsymbol{G}$ over some interface plane separating the bulk and surface regions. This result is very important conceptually for understanding surface electronic structure, but explicit wavefunction matching is rarely used in practise (apart from the pioneering work of Appelbaum & Hamann (1972, 1973) on Na (001)

PHILOSOPHICAL TRANSACTIONS OF THE ROYAL SOCIETY A MATHEMATICAL, PHYSICAL & ENGINEERING SCIENCES
PHILOSOPHICAL TRANSACTIONS OF THE ROYAL SOCIETY A MATHEMATICAL, PHYSICAL & ENGINEERING SCIENCES

Downloaded from rsta.royalsocietypublishing.org

and Si (111)). The usual approach in surface calculations is to use slab geometry, so that one is dealing with a system of finite thickness (typically five atomic layers thick) for which ordinary basis set methods can be used. Because quantities involving sums over states like charge density and energy are very local, the presence of the second surface of the slab does not matter for cohesive properties. However, for a precise description of individual electronic states, slab geometry is not adequate: in slab geometry, all the states at fixed $\boldsymbol{K}$ are discrete, and there is no real distinction between the discrete surface states localized at the surface, and bulk states bouncing off the surface. It is also unsatisfactory, perhaps, to solve the Schrödinger equation for two surfaces separated by a piece of bulk material, when all we want are the surface properties.

The 'surface embedded Green function method' (SEGF) provides a practical scheme for solving the Schrödinger equation for the surface of a real semi-infinite solid. As in wavefunction matching, this method assumes that the semi-infinite solid can be divided into two regions: region I which is the real surface region, say the top layer or two of atoms and the vacuum, and region II where an electron feels essentially the bulk potential. We then solve the Schrödinger equation explicitly only in the surface region, adding on to the hamiltonian a complex, energy-dependent embedding potential to describe the scattering of the electrons by the substrate region II.

To obtain the embedding potential (Inglesfield 1981), we start from the variational principle, with an arbitrary trial function $\phi(\boldsymbol{r})$ defined in region I. This trial function can in principle be extended into region II by finding the solution of the Schrödinger equation in this region at some trial energy ϵ, which matches onto ϕ in amplitude over the interface S between the two regions; let us call this ψ. The expectation value of the hamiltonian in the whole system is then:

$$E = \left[\int_{\mathrm{I}} \mathrm{d}^3\boldsymbol{r}\phi^*(\boldsymbol{r})\,H\phi(\boldsymbol{r}) + \epsilon\int_{\mathrm{II}} \mathrm{d}^3\boldsymbol{r}|\psi|^2 + \frac{1}{2}\int_{\mathrm{S}} \mathrm{d}^2\boldsymbol{r}_s\,\phi^*\frac{\partial\phi}{\partial n_s} - \frac{1}{2}\int_{\mathrm{S}} \mathrm{d}^2\boldsymbol{r}_s\,\phi^*\frac{\partial\psi}{\partial n_s}\right] \times\left[\int_{\mathrm{I}} \mathrm{d}^3\boldsymbol{r}|\phi|^2 + \int_{\mathrm{II}} \mathrm{d}^3\boldsymbol{r}|\psi|^2\right]^{-1}. \quad (1)$$

The surface integrals in (1) come from the discontinuity in the normal derivative of the trial function across S. The fundamental principle of embedding is that the integrals through the substrate region can be eliminated, using the Green function for the bulk crystal satisfying the boundary condition on S that:

$$\partial G_0(\boldsymbol{r}_s, \boldsymbol{r}')/\partial n_s = 0. \quad (2)$$

The inverse of G_0 over S is the generalized logarithmic derivative, relating the derivative of a solution of the Schrödinger equation in II to the amplitude:

$$\frac{\partial\psi(\boldsymbol{r}_s)}{\partial n_s} = -2\int_{\mathrm{S}} \mathrm{d}^2\boldsymbol{r}'_s\,G_0^{-1}(\boldsymbol{r}_s, \boldsymbol{r}'_s)\,\psi(\boldsymbol{r}'_s). \quad (3)$$

Substituting (3) into (1) and making use of a relationship between normalization integrals in II and the energy derivative of $\partial\psi/\partial n_s$ we finally obtain:

$$E = \left[\int_{\mathrm{I}} \mathrm{d}^3\boldsymbol{r}\phi^*(\boldsymbol{r})\,H\phi(\boldsymbol{r}) + \frac{1}{2}\int_{\mathrm{S}} \mathrm{d}^2\boldsymbol{r}_s\,\phi^*\frac{\partial\phi}{\partial n_s} + \int_{\mathrm{S}} \mathrm{d}^2\boldsymbol{r}_s\int_{\mathrm{S}} \mathrm{d}^2\boldsymbol{r}'_s\,\phi^*(\boldsymbol{r}_s)\left(G_0^{-1} - \epsilon\frac{\partial G_0^{-1}}{\partial\epsilon}\right)\phi(\boldsymbol{r}'_s)\right] \times\left[\int_{\mathrm{I}} \mathrm{d}^3\boldsymbol{r}|\phi|^2 + \int_{\mathrm{S}} \mathrm{d}^2\boldsymbol{r}_s\int_{\mathrm{S}} \mathrm{d}^2\boldsymbol{r}'_s\,\phi^*(\boldsymbol{r}_s)\frac{\partial G_0^{-1}}{\partial\epsilon}\phi(\boldsymbol{r}'_s)\right]^{-1}. \quad (4)$$

Downloaded from rsta.royalsocietypublishing.org

This expression gives us the expectation value of E purely in terms of the trial function ϕ defined in region I, and values of the embedding potential G_0^{-1} over S.

To find the actual wavefunction in the surface region we can now expand ϕ in terms of any suitable set of basis functions (we actually use linearized augmented plane waves, LAPWS (Krakauer *et al.* 1979)):

$$\phi(\boldsymbol{r}) = \sum_i a_i \chi_i(\boldsymbol{r}), \tag{5}$$

and minimizing E in (4) gives the matrix equation for the coefficients:

$$\sum_j \left[H_{ij} + (G_0^{-1})_{ij} + (E-\epsilon)\frac{\partial (G_0^{-1})_{ij}}{\partial \epsilon} \right] a_j = E \sum_j S_{ij} a_j. \tag{6}$$

The matrix elements are given by:

$$\left.\begin{aligned} H_{ij} &= \int_{\mathrm{I}} \mathrm{d}^3\boldsymbol{r} \chi_i^* H \chi_j + \frac{1}{2}\int_{\mathrm{S}} \mathrm{d}^2\boldsymbol{r}_s \chi_i^* \frac{\partial \chi_j}{\partial n_s}, \\ (G_0^{-1})_{ij} &= \int_{\mathrm{S}} \mathrm{d}^2\boldsymbol{r}_s \int_{\mathrm{S}} \mathrm{d}^2\boldsymbol{r}'_s \chi_i^* G_0^{-1} \chi_j, \\ S_{ij} &= \int_I \mathrm{d}^3\boldsymbol{r} \chi_i^* \chi_j. \end{aligned}\right\} \tag{7}$$

H_{ij} is the matrix element of the hamiltonian in region I, with the additional surface integral which ensures hermiticity. $(G_0^{-1})_{ij}$ is the matrix element of the embedding potential, evaluated at energy ϵ, and the energy derivative term in (6) is the first-order correction to give it at the right energy. The embedding potential is, in fact, a *pseudopotential* (Heine 1970) replacing the whole of region II: the relationship between the energy derivative of the embedding potential and the normalization of the wavefunction in the region of space which it is replacing is, of course, familiar from standard pseudopotential theory (Shaw & Harrison 1967).

In surface applications of the embedding method (Inglesfield & Benesh 1988) it is more convenient to evaluate the surface Green function rather than individual wavefunctions, because at a particular wavevector $\boldsymbol{K}$ the bulk states hitting the surface form a continuum. From the Green function we can immediately find the local density of states, which when integrated over energies up to E_{F} gives the charge density. To go to self-consistency we must solve Poisson's equation in the surface region with this charge density, with the boundary condition that the potential over interface S equals the bulk potential. Deep in the vacuum the boundary condition on the Hartree potential is that $\mathrm{d}V/\mathrm{d}z$ equals the applied electric field $\mathscr{E}$, and this is the only point at which the field enters the calculation (Aers & Inglesfield 1989).

3. Screening charge at Ag (001) and Al (001) surfaces

When an electric field is applied to a surface, the most striking feature of the resulting screening charge distribution is that it is located on top of the surface atoms, so that the field barely penetrates the solid. Figure 1 shows the screening charge at Ag (001) (Aers & Inglesfield 1989), calculated using the SEGF embedding method,

Downloaded from rsta.royalsocietypublishing.org

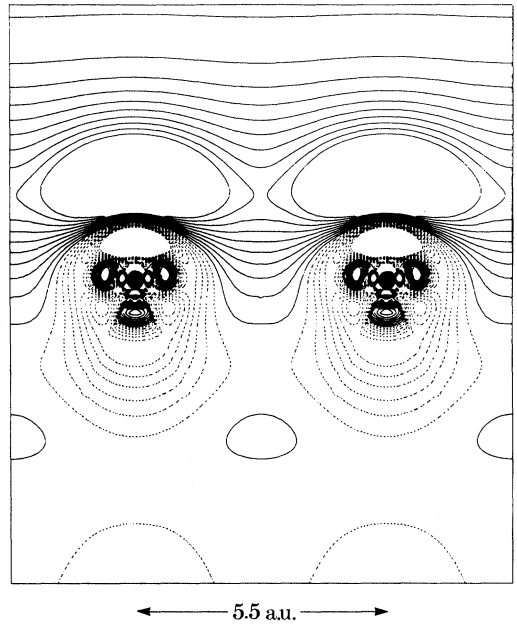

Figure 1. Screening charge at Ag (001) with field $\mathscr{E} = 0.01$ a.u. The plane passes through atoms in the top layer (indicated by heavy dots), and between atoms in the second layer; vacuum is at the top of the figure, and the bulk solid at the bottom. Solid lines are contours of decreased electron density, and dashed lines increased density.

with an applied field of $\mathscr{E} = +0.01$ a.u.† (5×10^9 V m^{-1}) (my convention is that a positive field repels electrons from the surface). There is atomic structure apparent in the screening charge, with polarization effects inside the ion cores; however, the main effect of the ion cores is to exclude the screening charge, which bends over the tops of the cores into the region between the atoms. The corresponding change in potential due to the application of the field is shown in figure 2; we see the equispaced potential contours outside the solid, but we also see how effective the screening charge is in excluding the field. This is relevant to field evaporation, as the force on an atom in an applied field is just the screened field at the nucleus, from the Hellmann–Feynman theorem; we explore this further in §4.

The shape of the screening charge is field-dependent, corresponding to nonlinear screening. In figure 3 we show the planar averaged screening charge as a function of z, the distance from the geometrical surface (where the solid is chopped in two), for fields of ± 0.02 a.u. at Ag (001). We see that an increasing positive field tends to push the screening charge into the solid, whereas an increasing negative field tends to pull it out. From our results we find that the centre of gravity of this screening charge distribution, as a function of $\mathscr{E}$, can be quite well fitted by the straight line:

$$z_0 = -0.97 + 8.83\mathscr{E} \quad \text{(in atomic units)}. \tag{8}$$

The zero-field value of z_0 is the electrostatic origin of the surface, from which the asymptotic form of the image potential should be measured; so at Ag (001) the image plane lies at -0.97 a.u., on the *vacuum* side of the geometrical surface.

† 1 a.u. $\approx 5.3 \times 10^{-11}$ m.

Downloaded from rsta.royalsocietypublishing.org

Figure 2

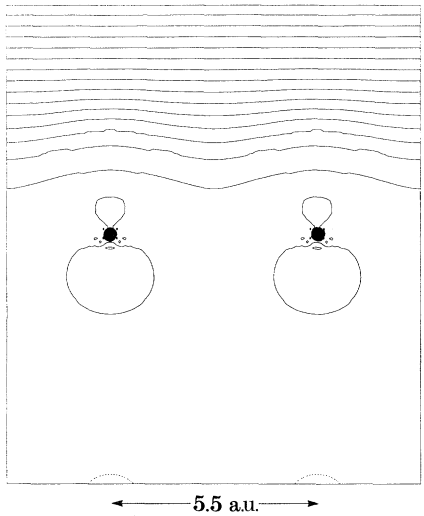

Figure 3

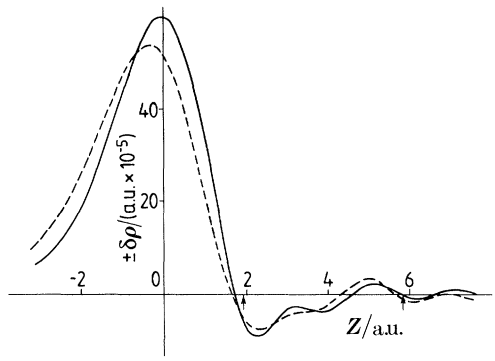

Figure 2. Change in potential at Ag (001) with field $\mathscr{E} = 0.01$ a.u.

Figure 3. Planar-averaged screening charge at Ag (001) for fields $\mathscr{E} = +0.02$ a.u. (solid line), and $\mathscr{E} = -0.02$ a.u. (dashed line), as a function of distance from the geometrical surface. Arrows mark the surface and subsurface atomic planes.

Our calculated image plane can be compared with the results of inverse photoemission experiments. By treating z_0 as a parameter in a model surface potential and using this to fit the experimentally observed energies of the Rydberg surface states, Smith *et al.* (1989) conclude that the image plane at Ag (001) lies at $+0.18$ a.u., on the *solid* side of the surface. Our result is in marginally better agreement with experiment than the jellium result (Weber & Liebsch 1987*a*), $z_0 = -1.35$ a.u., found using jellium of density $r_s = 3$ a.u., which is frequently used to model the response of Ag surfaces to external fields. However, there does seem to be a real discrepancy between our theory and experiment – what might the reasons for this be? From (8), nonlinear effects – due to the size of the electric field produced by the electron in the surface state – are not big enough to account for the discrepancy. A fundamental problem is that the calculation is carried out within the local density approximation, which does not correctly describe the image potential in the Schrödinger equation. Several authors have tried to improve on this for jellium: Ossicini *et al.* (1987) used the non-local exchange-correlation potential of the weighted density approximation in their determination of the screening charge, and Serena *et al.* (1988) used an interpolation scheme between the asymptotic form of the image potential and the local density potential nearer the surface. For jellium with $r_s = 3$ a.u. these corrections push the image plane 0.1 a.u. closer to the surface. However, the real problem is that our calculation gives the response of the surface to a static external charge, whereas an electron in a Rydberg surface state is a dynamic object. We ought, in fact, to be calculating the asymptotic form of the *self-energy* (Inkson 1971).

The position of the image plane at Al surfaces has been calculated by several authors, and it provides a sensible system for comparison with the jellium results of Lang & Kohn (1973): for $r_s = 2$ a.u., $z_0 = -1.6$ a.u. We find that the centre of gravity of the screening charge for Al (001) in an electric field of $+0.01$ a.u. lies at $z_0 =$

Downloaded from rsta.royalsocietypublishing.org

−1.1 a.u., significantly closer in than for jellium. In their pseudopotential slab calculation, in which the z-dependent planar-averaged potential was used, Serena *et al.* (1988) find the image plane 0.26 a.u. closer in to the surface than the jellium result. Another comparison is with the work of Finnis (1990), who puts the image plane for Al (111) at −0.87 a.u. Although there are discrepancies between the different calculations, it appears that the image plane lies closer to the surface when atoms are included than in the jellium calculation. The reason for this is that the electrons feel a more attractive electrostatic potential than in jellium, where the bulk electrostatic potential from the electrons and compensating positive background is zero. The more attractive potential reduces the spilling-out of the electrons at the surface, hence pulls in the image plane.

The field-dependence of the screening charge profile gives a second-order current normal to the surface, and the intensity of the second harmonic reflected from the surface in a low-frequency external field is proportional to the square of the coefficient of $\mathscr{E}$ in (8) (Weber & Liebsch 1987*a*). This is of considerable interest nowadays, because second harmonic generation is very surface-sensitive, and can be greatly enhanced by small quantities of alkali adsorbates for example (Weber & Liebsch 1987*b*). Our results show that the screening charge at the Ag (001) surface is much stiffer than jellium calculations indicate: our value of 8.83 for the coefficient of $\mathscr{E}$ in (8) is to be compared with the value of 30 a.u. found for jellium with $r_s =$ 3 a.u. In other words, we predict a second harmonic intensity a factor of 12 smaller than for a jellium model of Ag (001). This is in the right direction to obtain agreement with experiment, as Guyot-Sionnest *et al.* (1990) have shown in a recent study of a Ag electrode–electrolyte interface. A possible explanation for the greater stiffness of the screening charge in the Ag (001) calculation is that the ion cores seem relatively impenetrable (figure 1), thereby pinning the screening charge.

4. Surface effective charges

The force normal to the surface on atoms i in an external electric field $\mathscr{E}$ can be used to define their effective charge:

$$F_i = q_i^* \mathscr{E}. \tag{9}$$

From Hellmann–Feynman, F_i is the fully screened field at nucleus i times the nuclear charge, so q_i^* is a measure of the effectiveness of the screening; from the results for the screened potential shown in figure 2 we would expect q_i^* to be normally rather small. As elementary electrostatics tell us that the total force on the surface is proportional to $\mathscr{E}^2$ and the force linear in $\mathscr{E}$ vanishes, it follows that:

$$\sum_i q_i^* = 0, \tag{10}$$

a result discussed many years ago by Trullinger & Cunningham (1973).

The surface effective charge gives the variation in work-function ϕ with atomic displacements (Hamann 1987). Let us consider the variation $\delta\phi$ when all atoms of type i (this will be a layer of atoms parallel to the surface) are displaced by δz normal to the surface. As the work-function is given by the energy change in removing an electron through the surface to infinity, we can write $\delta\phi$ as:

$$\delta\phi = (\partial E_{N-1}/\partial z_i - \partial E_N/\partial z_i)\,\delta z_i, \tag{11}$$

where E_N is the energy of the charge-neutral system with N electrons, and E_{N-1} is the

Downloaded from rsta.royalsocietypublishing.org

Table 1

external field (a.u.)	field at H (a.u.)
0	−0.004431
0.005	−0.004327
0.01	−0.004358
0.02	−0.004261

energy of the charged system with one electron removed. Now $\partial E_N/\partial z_i$ is zero in equilibrium, and $\partial E_{N-1}/\partial z_i$ is (minus) the force on the $\mathcal{N}$ atoms of type i in the charged system. But in this charged system (we assume it is metallic), the charge deficit is at the surface, so there is an external field given by:

$$\mathscr{E} = -4\pi|e|/\mathcal{N}A, \tag{12}$$

where A is the area of the surface unit mesh. Hence we obtain the connection between the work-function variation and the effective charge:

$$\partial\phi/\partial z_i = 4\pi q_i^*/A. \tag{13}$$

In this expression the convention is that the electronic charge is negative, and z is directed into the surface. As the variation in work-function with atomic displacement comes entirely from the change in the surface dipole layer, this expression has just the form we would expect from moving charges q_i^* rigidly, and it is analogous to the standard theory of effective charges in ionic crystals.

With a surface phonon, the variation of the surface dipole over the surface via (13) sets up long-range electric fields which scatter electrons in EELS experiments (Ibach 1971). An interesting case is a monolayer of H on Rh (001), where EELS experiments show evidence of dipole-active modes, corresponding to a finite effective charge on the H atoms (Richter & Ho 1987). However, Hamann & Feibelman (1988) found in a slab calculation, with H adsorbed on either side of a 3-layer Rh (001) film, that the work-function is remarkably constant as a function of the H–Rh interlayer spacing, suggesting an effective charge of zero! To try to resolve this, we have carried out an embedded calculation for Rh (001) (1×1)–H, treating explicitly the H and the top layer of Rh, and embedding this on to bulk Rh (Miller & Inglesfield 1991). As we have seen, embedding eliminates the finite size effects associated with the slab. From the change in work-function around the equilibrium interlayer spacing (1.1 a.u. with the H atoms in four-fold hollow sites), we find that the effective charge on the H atoms is $+0.009|e|$. Next, we determined the effective charge from (9), applying an electric field to the surface and finding directly the screened field at the H nucleus. Our results, presented in table 1, show considerable scatter, and in the case of zero external field there is actually a field at the H due to the fact that one layer of Rh is not enough to do the equilibrium energetics accurately. Nevertheless, a straight line of slope $+0.009$ – corresponding to the effective charge of $+0.009|e|$ – provides a reasonable fit.

This effective charge for H atoms adsorbed on Rh (001) is much smaller than is found on other substrates: $q_{\mathrm{H}}^* = +0.054|e|$ for H/Pd (111) and $-0.032|e|$ for H/W (001) (Hamann 1987), and it remains to be seen whether it is compatible with the EELS results. This substrate dependence is not just a question of electronegativity, because Rh and Pd are the same on the Pauling scale; we do find a structure dependence to the effective charge (Miller & Inglesfield 1990).

PHILOSOPHICAL TRANSACTIONS OF THE ROYAL SOCIETY A MATHEMATICAL, PHYSICAL & ENGINEERING SCIENCES

PHILOSOPHICAL TRANSACTIONS OF THE ROYAL SOCIETY A MATHEMATICAL, PHYSICAL & ENGINEERING SCIENCES

Downloaded from rsta.royalsocietypublishing.org

5. Effective charges and surface instability

A large effective charge can lead to a surface instability. This was first shown by Trullinger & Cunningham (1973) using a pair force expression for the dynamical matrix, including long-range Coulomb forces between the effective charges, but we shall use a more general, macroscopic argument.

We consider a normal displacement of atom i, as in (13), but with an amplitude varying sinusoidally over the surface with wavevector $\boldsymbol{K}$:

$$\delta z_i(\boldsymbol{R}) = a_i \sin(\boldsymbol{K}\cdot\boldsymbol{R}). \tag{14}$$

From (13), this sets up a spatially varying surface barrier potential, and because the bulk Fermi energy is constant, the electrostatic potential outside the surface varies as:

$$V(\boldsymbol{R}, z) = -(4\pi/A)\, q_i^*\, a_i \sin(\boldsymbol{K}\cdot\boldsymbol{R}) \exp(Kz). \tag{15}$$

The normal component of the corresponding 'patch' electric field near the surface is:

$$\mathscr{E} = (4\pi/A)\, q_i^*\, K a_i \sin(\boldsymbol{K}\cdot\boldsymbol{R}), \tag{16}$$

so from (9) the force on the atoms is:

$$F = (4\pi/A)\,(q_i^*)^2 K a_i \sin(\boldsymbol{K}\cdot\boldsymbol{R}), \tag{17}$$

proportional to the displacements of the atoms, and countering the local restoring forces. If the restoring force on atoms i in the long-wavelength limit is α_i, we see that the surface is unstable for displacement wavelengths shorter than

$$\lambda = 8\pi^2 (q_i^*)^2/\alpha_i A. \tag{18}$$

This suggests that any surface with non-vanishing q_i^* will be unstable for sufficiently short wavelengths, but of course the argument breaks down once λ is of the order of an interatomic spacing.

It was suggested by Trullinger & Cunningham (1973) that an effective-charge-driven instability might be responsible for semiconductor surface reconstructions. However, it is the dangling bonds which drive the reconstructions in these cases. But one candidate for such a reconstruction is O adsorbed on Cu (001), the $(\sqrt{2}\times\sqrt{2})R45°$ structure, with O atoms in four-fold hollow sites suggested by analogy with O/Ni (001), is unstable (Asensio *et al.* 1990). From our calculations (Colbourn & Inglesfield 1991), the effective charge of the O atoms in these ideal sites is $-0.9|e|$. Taking the force constant from EELS measurements (Wuttig *et al.* 1989) as 0.072 a.u. we find that the surface is unstable for wavelengths smaller than 19 a.u. But this is considerably greater than the O–O interatomic spacing, so the surface must be unstable in the ideal structure.

I have had very useful discussions on effective charges with Wolfram Miller and Elizabeth Colbourn. The work has been supported by FOM (Stichting voor Fundamenteel Onderzoek der Materie).

References

Aers, G. C. & Inglesfield, J. E. 1989 Electric fields and Ag (001) surface electronic structure. *Surf. Sci.* **217**, 367–383.

Appelbaum, J. A. & Hamann, D. R. 1972 Self-consistent electronic structure of solid surfaces. *Phys. Rev.* B**6**, 2166–2177.

Appelbaum, J. A. & Hamann, D. R. 1973 Surface states and surface bonds of Si (111). *Phys. Rev. Lett.* **31**, 106–109.

Asensio, M. C., Ashwin, M. J., Kilcoyne, A. L. D., Woodruff, D. P., Robinson, A. W., Lindner, Th.,

Downloaded from rsta.royalsocietypublishing.org

Somers, J. S., Ricken, D. E. & Bradshaw, A. W. 1990 The structure of oxygen adsorption phases on Cu (100). *Surf. Sci.* **236**, 1–14.

Colbourn, E. A. & Inglesfield, J. E. 1991 Surface instability and electronic structure of O on Cu (001). (In preparation.)

Finnis, M. W. 1990 The interaction of a point charge with an aluminium (111) surface. *Surf. Sci.* (In the press.)

Fu, C. L. & Ho, K. M. 1989 External-charge-induced surface reconstruction on Ag (110). *Phys. Rev. Lett.* **63**, 1617–1620.

Guyot-Sionnest, P., Tadjeddine, A. & Liebsch, A. 1990 Electronic distribution and non-linear optical response at the metal-electrolyte interface. *Phys. Rev. Lett.* **64**, 1678–1681.

Hamann, D. R. 1987 Hydrogen vibrations at transition metal surfaces. *J. Elect. Spectroscopy* **44**, 1–16.

Hamann, D. R. & Feibelman, P. J. 1988 Anharmonic vibrational modes of chemisorbed H on the Rh (001) surface. *Phys. Rev.* B **37**, 3847–3855.

Heine, V. 1963 On the general theory of surface states and scattering of electrons in solids. *Proc. Phys. Soc.* **81**, 300–310.

Heine, V. 1970 The pseudopotential concept. *Solid St. Phys.* **24**, 1–36.

Ibach, H. 1971 Surface vibrations of silicon detected by low-energy electron spectroscopy. *Phys. Rev. Lett.* **27**, 253–256.

Inglesfield, J. E. 1981 A method of embedding. *J. Phys.* C **14**, 3795–3806.

Inglesfield, J. E. 1990 Electric fields and surface electronic structure. *Vacuum* **41**, 543–546.

Inglesfield, J. E. & Benesh, G. A. 1988 Surface electronic structure: embedded self-consistent calculations. *Phys. Rev.* B **37**, 6682–6700.

Inkson, J. C. 1971 The electron–electron interaction near an interface. *Surf. Sci.* **28**, 69–76.

Kolb, D. M., Boeck, W., Ho, K.-M. & Liu, S.-H. 1981 Observation of surface states on Ag (100) by infrared and visible electroreflectance spectroscopy. *Phys. Rev. Lett.* **47**, 1921–1924.

Krakauer, H., Posternak, M. & Freeman, A. J. 1979 Linearized augmented plane-wave method for the electronic band structure of thin films. *Phys. Rev.* B **19**, 1706–1719.

Lang, N. D. & Kohn, W. 1970 Theory of metal surfaces: charge density and surface energy. *Phys. Rev.* B **1**, 4555–4568.

Lang, N. D. & Kohn, W. 1973 Theory of metal surfaces: induced surface charge and image potential. *Phys. Rev.* B **7**, 3541–3550.

Liebsch, A. & Schaich, W. L. 1989 Second-harmonic generation at simple metal surfaces. *Phys. Rev.* B **40**, 5401–5410.

Melmeed, A. J., Tung, R. T., Graham, W. R. & Smith, G. D. W. 1979 Evidence for reconstructed (001) tungsten obtained by field-ion microscopy. *Phys. Rev. Lett.* **43**, 1521–1524.

Miller, W. & Inglesfield, J. E. 1991 Effective charge of H on Rh (001). (In preparation.)

Ossicini, S., Finocchi, F. & Bertoni, C. M. 1987 Electron density profiles at charged metal surfaces in the weighted density approximation. *Surf. Sci.* **189/190**, 776–781.

Richter, L. J. & Ho, W. 1987 Vibrational modes of hydrogen adsorbed on Rh (100) and their relevance to desorption kinetics. *J. Vac. Sci. Technol.* A **5**, 453–454.

Serena, P. A., Soler, J. M. & Garcia, N. 1988 Work function and image-plane position of metal surfaces. *Phys. Rev.* B **37**, 8701–8706.

Shaw, R. W. Jr & Harrison, W. A. 1967 Reformulation of the screened Heine–Abarenkov model potential. *Phys. Rev.* **163**, 604–611.

Smith, N. V., Chen, C. T. & Weinert, M. 1989 Distance of the image plane from metal surfaces. *Phys. Rev.* B **40**, 7565–7573.

Trullinger, S. E. & Cunningham, S. L. 1973 Soft-mode theory of surface reconstructions. *Phys. Rev. Lett.* **30**, 913–916.

Weber, M. G. & Liebsch, A. 1987*a* Density-functional approach to second-harmonic generation at metal surfaces. *Phys. Rev.* **35**, 7411–7416.

Weber, M. G. & Liebsch, A. 1987*b* Theory of second-harmonic generation by metal overlayers. *Phys. Rev.* B **36**, 6411–6414.

PHILOSOPHICAL TRANSACTIONS OF THE ROYAL SOCIETY A MATHEMATICAL, PHYSICAL & ENGINEERING SCIENCES

PHILOSOPHICAL TRANSACTIONS OF THE ROYAL SOCIETY A MATHEMATICAL, PHYSICAL & ENGINEERING SCIENCES

Downloaded from rsta.royalsocietypublishing.org

Wuttig, M., Franchy, R. & Ibach, H. 1989 Oxygen on Cu (100) – a case of an adsorbate induced reconstruction. *Surf. Sci.* **213**, 103–136.

Discussion

D. Weaire (*Dublin, Republic of Ireland*). The embedding method really comes into its own for SHG because a finite slab must have two surfaces, whose contributions can actually cancel in a naive calculation! How does Professor Inglesfield calculate the SHG from the single surface in his formation?

J. E. Inglesfield. This is calculated from the field dependence of the shape of screening charge, in the response of the surface to an external field. At the moment it is only possible to calculate static response when a real surface is treated, so the calculation is really only applicable in the low-frequency limit; it cannot treat spectroscopic aspects of SHG.

O. K. Andersen (*Stuttgart, F.R.G.*). At the meeting we have heard a lot about pseudopotentials and local density functional potentials. The advantage of such potentials is that they are energy independent, local in r-space, weak, etc. Professor Inglesfield's surface electronic structure method uses a so-called embedding potential to describe the semi-infinite bulk part of the system, but in his talk he did not tell us about the properties and the advantages of using this potential. Is it not strongly energy dependent, non-local and so on? How does Professor Inglesfield's method compare with Green's function techniques (e.g. matching – or Dyson's – methods)?

J. E. Inglesfield. The embedding potential is non-local, energy dependent and complex; inevitably non-local because it is describing the scattering properties of the whole substrate, energy dependent because this is connected with the normalization of the wavefunctions in the substrate, and complex to smear out the discrete states of the finite surface region into the continuum associated with the semi-infinite solid.

We have compared embedding results with Pollmann's work on Si (001) using a Dyson's equation approach and found good agreement; embedding offers greater freedom in the choice of basis set, but this is not always an advantage. It has an advantage over matching Green function methods once the embedding potential has been determined, because embedding methods can use fairly standard band structure technology.

U. Gerhardt (*Frankfurt, F.R.G.*). The system oxygen on Cu (001) is a very tricky one. We actually found out by LEED investigations that the adsorption site on a very smooth Cu (001) surface, i.e. one without surface steps, is the bridge site. The fourfold hollow site only shows up if such steps are present. This might, however, be compatible with the surface instability mentioned after all.

J. E. Inglesfield. This is a very interesting result; I cannot deduce, from my surface instability argument, what the surface will go to. Clearly O on Cu (001) is a very difficult and remarkable surface.

V. Heine (*Cambridge, U.K.*). The essence of jellium to my mind is that the potential in the bulk is a constant. The question is what value to take for that constant. If we

PHILOSOPHICAL TRANSACTIONS OF THE ROYAL SOCIETY A MATHEMATICAL, PHYSICAL & ENGINEERING SCIENCES

Downloaded from rsta.royalsocietypublishing.org

start from a pseudopotential picture of a real metal, then one should take the mean Hartree pseudopotential. Unfortunately in the jellium calculations done by most people, the Hartree potential is effectively set equal to zero, which seems to me physically quite unrealistic as a model of real metal. In both cases the (attractive) exchange and correlation potential is added: in my approach one must be careful not to count that twice. Of course in the infinite bulk solid it makes no difference which one does: indeed there is no way of defining a zero of potential. But at a surface the difference between the two jellium models is quite significant, and I am therefore not surprised by the difference in the second-order response to a surface electric field that was mentioned.

PHILOSOPHICAL TRANSACTIONS OF THE ROYAL SOCIETY A MATHEMATICAL, PHYSICAL & ENGINEERING SCIENCES

PHILOSOPHICAL TRANSACTIONS OF THE ROYAL SOCIETY A MATHEMATICAL, PHYSICAL & ENGINEERING SCIENCES